HHS Public Access

Author manuscript

Eur J Neurosci. Author manuscript; available in PMC 2017 February 01.

Published in final edited form as:

Eur J Neurosci. 2016 February ; 43(3): 451–462. doi:10.1111/ejn.13059.

Lack of motor recovery after prolonged denervation of the neuromuscular junction is not due to regenerative failure

Miyuki Sakuma[1], **Grzegorz Gorski**[1], **Shu-Hsien Sheu**[2], **Stella Lee**[1], **Lee B. Barrett**[1], **Bhagat Singh**[1], **Takao Omura**[1], **Alban Latremoliere**[1], and **Clifford J. Woolf**[1]

[1]F.M. Kirby Neurobiology Center, Boston Children's Hospital and Department of Neurobiology, Harvard Medical School, Boston, 02115 MA, USA

[2]Department of Pathology and Department of Cardiology, Boston Children's Hospital and Department of Neurobiology, Harvard Medical School, Boston, 02115 MA, USA

Abstract

Motor axons in peripheral nerves have the capacity to regenerate after injury. However, full functional motor recovery rarely occurs clinically, and this depends on the nature and location of the injury. Recent preclinical findings suggest that there may be a time after nerve injury where, while regrowth to the muscle successfully occurs, there is nevertheless a failure to reestablish motor function, suggesting a possible critical period for synapse reformation. We have now examined the temporal and anatomical determinants for the reestablishment of motor function after prolonged neuromuscular junction (NMJ) denervation in rats and mice. Using both sciatic transection-resuture and multiple nerve crush models in rats and mice to produce prolonged delays in reinnervation, we show that regenerating fibers reach motor endplates and anatomically fully reform the NMJ even after extended periods of denervation. However, in spite of this remarkably successful anatomical regeneration, after 1 month of denervation there is a consistent failure to reestablish functional recovery, as assessed by behavioral and electrophygiological assays. We conclude that this represents a failure in reestablishment of synaptic function, and the possible mechanisms responsible are discussed, as are their clinical implications.

Graphical abstract

Correspondence: Dr. Clifford J Woolf or Dr. Alban Latremoliere. Clifford.woolf@childrens.harvard.edu or alban.latremoliere@childrens.harvard.edu.

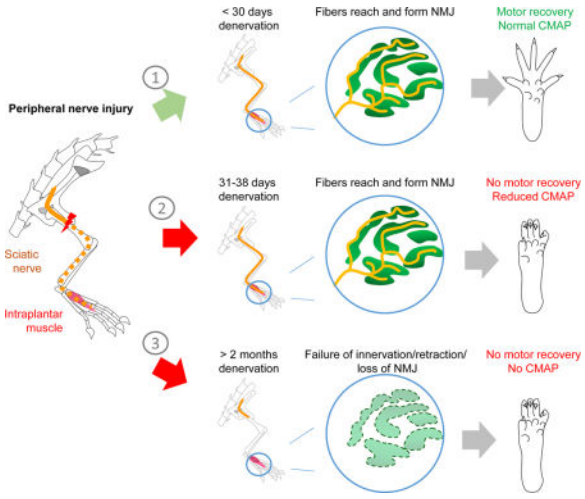

Keywords

Neuromuscular junction; regeneration; peripheral nerve injury; motor functional recovery; critical period

Introduction

Peripheral nerve injuries represent a significant source of patient morbidity and disability (Asplund *et al.*, 2009; Kawamura *et al.*, 2010). Although advances in surgical procedures, such as nerve autografts (Millesi *et al.*, 1972), nerve transfer (Tsuyama *et al.*, 1969), partial nerve transfer (Oberlin *et al.*, 1994) and direct spinal root implantation (Carlstedt *et al.*, 1995) have led to improvement in surgical results, nerve repairs result in only a 51.6% satisfactory motor recovery (Ruijs *et al.*, 2005). Furthermore, proximal injuries and delayed interventions are generally met with poor functional outcomes (Hoke, 2006). This is in marked contrast to the successful restoration of motor function that occurs in the standard rodent model of sciatic nerve crush, where a full recovery occurs within several weeks.

The prevalent hypothesis for this dichotomy is that axons of human motor neurons must regenerate over much longer distances than rodents to reach their target, the neuromuscular junction (NMJ), despite a similar growth rate of ~1–2 mm per day (Buchthal & Kuhl, 1979; Griffin *et al.*, 2010). Consequently this means there is a considerable delay of many months or even longer in patients before muscles may be potentially reinnervated, in contrast to the rapid reinnervation possible in rodents.

The failure of motor recovery after long-term denervation (> 6 months) has been attributed to a failure of axons to reach the target (Fu and Gordon 1995) even though injured motor neurons maintain an intrinsic capacity to grow even after extended times (up to 12 months; Fu & Gordon, 1995; Terenghi, 1999; Saito & Dahlin, 2008). Changes in the denervated nerve and muscle are thought to progressively make the distal milieu increasingly non-permissive for growth (Sulaiman & Gordon, 2000) and even promote axonal retraction (Luo

& O'Leary, 2005; Gallo, 2006), such that too long a delay (>12 weeks) is thought to prevent regeneration to the NMJ.

Following a peripheral nerve injury Schwann cells distal to the axotomy dedifferentiate into a pro-regenerative state, where they produce large amounts of growth factors such as glial cell-line-derived neurotrophic factor (GDNF) in the denervated nerve (Jessen & Mirsky, 2002). This gradually decreases though over time in chronically denervated distal nerve segments and eventually there is a failure to produce sufficient levels of trophic factors to support nerve growth after 12 weeks (Fu & Gordon, 1997; Hoke *et al.*, 2002). While terminal Schwann cells located in the NMJ guide regenerating axons to denervated endplates through an extension of processes that start a few days following nerve injury (Reynolds & Woolf, 1992; Son & Thompson, 1995), they start retracting their processes from the endplates after prolonged denervation, >5 weeks, decreasing the capacity for reinnervation by re-growing motor fibers (Kang *et al.*, 2014). After very prolonged denervation (6 months) Schwann cells eventually atrophy and the basal lamina and bands of Büngner degenerate (Vuorinen *et al.*, 1995), physically removing tracks for axonal growth. Extensive delays of many months results, therefore, in progressive obstacles to axon regrowth to muscle.

We recently showed in mice that even before the milieu becomes non-permissive by virtue of prolonged periods of denervation (3 to 6 months), there is at shorter time periods (~ 5 weeks) a critical period for successful motor recovery. We found following a sciatic nerve transection with resuture that while regenerating motor fibers eventually reached the NMJ, this was not associated with a positive functional outcome in distal muscles (Ma *et al.*, 2011). Motor functional recovery essentially plateaued after approximately 35 days post-injury, with no further improvement beyond this period, even though axons muscles were fully re-innervated (Ma *et al.*, 2011). We proposed that the failure might be due to a lack of full reinnervation of the NMJ – the axons got to the NMJ but appeared not to form the normal presynaptic apparatus.

We have now reexamined the timeframe of this critical period in rats as well as mice, using transection resuture and repeated crush approaches to delay axon regrowth down the distal segment. Furthermore, we have characterized by confocal light and electron microscopy of the NMJ, the extent of reinnervation in more detail, and have surveyed functional recovery by electromyography.

We confirm that regenerating fibers can fully reinnervate distal muscles even after several weeks of denervation and now show that they reestablish a structurally sound NMJ. However, these reformed NMJs are incapable of normally activating muscles, reflecting a synaptic rather than a regenerative failure.

Material and Methods

Animals and procedures

Animal care was in full accordance with the IACUC guidelines of Boston Children's Hospital. Male Sprague Dawley rats (200–250g; Charles River) or C57Bl6j mice (8–10

weeks; Jackson laboratories) were used. after at least 1week of habituation animals were randomized for experimental group and surgical procedures were performed under isoflurane anesthesia (3% induction/2% maintenance). The left sciatic nerve was exposed just below the sciatic notch under sterile conditions and then either crushed using Dumont #5/45 forceps for 30 seconds or transected and immediately repaired with 10-0 nylon under microscope. After the nerve injury, the incision wound was sutured and animals were allowed to recover on heated pads before being returned to their home cage.

Behavioral tests

All behavior experiments were conducted in a blinded fashion in a quiet room (temperature 22°C ± 1°C) from 9 AM to 6 PM.

For sensory recovery, an Austerlitz pin (0 for rats and 000 for mice; Fine Scientific Tools, USA) was used to assess high threshold mechanical sensitivity responsiveness of animals after nerve injury. Rats or mice were placed on wire mesh cages and tested after a 30-minute habituation period. The Austerlitz pin was gently applied to the plantar surface of the paw without moving the paw or penetrating the skin. The most lateral part of the plantar surface of the hind paw (sensory field of the sciatic nerve) was divided into 5 areas. The pinprick was applied from the most lateral toe to the heel. A response was considered positive when the animal briskly removed its paw, and the animal was graded 1 for this area, and then tested for the next one. If none of the applications elicited a positive response, the overall grade was 0. In that case, the saphenous territory of the same paw was tested as a positive control, which always elicited a positive response.

For motor recovery in rats, animals were recording walking (18 cm/sec) using DigiGait apparatus (Mouse Specifics, MA, USA) and sciatic nerve functional index (SFI) was calculated using the following formula:

$$\mathrm{SFI}=-38.3*(\mathrm{Lt}-\mathrm{Rt\ PL})/\mathrm{Rt\ PL}+109.5*(\mathrm{Lt}-\mathrm{Rt\ ITS})/\mathrm{Rt\ ITS}+13.3*(\mathrm{Lt}-\mathrm{Rt\ TS})/\mathrm{Rt\ T}-8.8$$

For motor recovery in mice, grip strength and toes spreading score were used. For grip strength mice were trained to grip the bar of the apparatus (Bioseb, France) with their hind limbs, and then, they were pulled off the bar horizontally. Each measurement was performed six times, and the force used to grip the bar was recorded in grams. For toes spreading score mice were gently covered with a piece of cloth and lifted by the tail, uncovering the hind paws for clear observation. Under this condition, the digits spread, maximizing the space between them (the toe spreading reflex). The reappearance of this reflex results from reinnervation of the small muscles of the foot and was scored as previously described (Ma *et al.*, 2011): 0, no spreading; 1, intermediate spreading with all toes; and 2, full spreading.

Electrophysiological examination

Rats were deeply anesthetized by an intra-peritoneal injection of urethane (200 mg/kg). Sciatic nerves were exposed bilaterally and a steel bipolar stimulating electrode placed under the sciatic nerve at the proximal level of sciatic notch. The recording electrode was placed in either the gastrocnemius muscle or the intraplantar muscle, a reference electrode

was placed distal to the recording electrode and a ground electrode was placed in the lower thigh. Compound muscle action potentials (CMAP) evoked by supramaximal square-wave stimulus pulses were recorded using a MEB-9400A-L-T EMG/NCV/EP system (Nihon Kohden, Foothill Ranch, CA). Amplitude, area, duration of compound muscle action potentials and the distal motor latency were measured.

Immunohistochemistry

Animals were perfused with 4% paraformaldehyde dissolved in PBS, and sciatic nerves, gastrocnemius and intraplantar muscles were dissected, postfixed, cryoprotected, and frozen in OCT (Tissue-Tek). 10 μm (sciatic nerve) or 20 μm (muscle) thick cryosections were blocked with 1% bovine serum albumin (Sigma-Aldrich)/0.1%Triton X-100 in 0.1 M phosphate buffered saline (PBS) and then incubated with anti-NF200 antibodies (1:2000, Millipore AB5220) overnight at 4°C. Muscle samples were co-incubated with FITC-conjugated Bungarotoxin (1:1000, life technology. B-13422). After 3 washes in PBS for 10 minutes each, sections were then incubated with secondary antibody (anti-chicken; 1:500 Jackson Immunoresearch laboratories) for 1 hour at room temperature, washed 3 times in PBS (10 minutes each) and mounted using Vectashield (H-1000). For fast and slow Myosin stainings cryosections were incubated in citrate buffer for antigen retrieval. After 3 washes in 0.5% Triton-X-100/1x PBS (5 minutes each at room temperature), the slides were incubated in Blocking Solution (Vector Labs FMK-2201, according to manufacturer's recommendations) for 45 minutes at room temperature. Slides were then incubated with anti-Myosin (Skeletal, Fast) antibody (1:100, Sigma-Aldrich M1570) and anti-Myosin (Skeletal, Slow) antibody (1:2000, Sigma-Aldrich M8421) for 1 hour at room temperature then washed with 0.1% Triton-X-100/1xPBS for 5 minutes. Slides were then incubated with the secondary antibody (1:200 goat anti–mouse Jackson Immunoresearch laboratories) for 1 hour in a foil-covered box followed by 3 washes in 0.1% Triton-X-100/1xPBS each 5 minutes and 1 wash in distilled water for 5 minutes at room temperature. Finally tissues were covered with Vectashield Mouting medium (H-1200) and placed glass coverslip on the tissue section slides. Images of sciatic nerve and muscle fiber staining were captured with NIKON ECLIPSE 80i microscope and NIKON DS-Qi1MC camera (4x) by NIS-Elements AR 3.10 software and axon number quantification was performed with ImageJ. Images of neuromuscular junctions were captured with Zeis LSM 700 confocal microscope and (64x) by ZEN 2009 software and the regenerated axons were quantified with Image J. Scoring of NMJ was performed by 2 experimenters blind to the experimental condition. Initial scoring was performed with the following criteria: fully, partially or non-innervated. The 'partially innervated' condition however showed high inter-experimenter variability and 'fully innervated' and 'partially innervated' were therefore pooled as one condition.

Hematoxylin and eosin staining

Animals were perfused with 4% paraformaldehyde dissolved in PBS, and sciatic nerves, gastrocnemius and intraplantar muscles were dissected and postfixed overnight. Samples were embedded in paraffin and sectioned at 8 μm. Slides were washed in Xylene for 5 minutes followed by two washes in 100% ethanol (5 minutes) and 95% ethanol (2x 5 minutes). Tissues were then dipped in distilled water for 2 minutes, and immersed for 10 minutes in Harris Hematoxylin. After that sections were differentiated in 1% acid alcohol

for 30 seconds, quickly washed in water for 1 minute, and bluined in 0.2% ammonia water for 30 seconds before a 3 minutes rince in tap water. After that sections were quickly immersed in 95% ethanol (1 minute) and stained in eosine solution for 1 minute. Slides were then dehydrated by successive incubations in 95% ethanol, 100% ethanol and xylene (two incubations of 4 minutes at each step) and mounted using cytoseal. Images of muscle staining were captured with NIKON ECLIPSE 80i microscope and NIKON DS-Qi1MC camera (4x) by NIS-Elements AR 3.10 software.

Electron microscopy

Animals were perfused transcardially with 0.1M sodium cacodylate buffer, pH 7.4, followed by the same buffer containing 2% PFA and 3% glutaraldehyde. Intraplantar muscles were removed and fixed overnight at room temperature in the same fixative. Muscles were washed with cacodylate buffer and stained en bloc in 1% osmium tetroside, 1% ferrocanide in cacodylate buffer for 5 h, washed with water, and then stained in 1% aqueous uranyl acetate for 2h. Muscles were dehydrated in graded alcohols and acetone, then embedded in Epon 812. Sections were mounted on formvarcoated Synptek slot grids (Electron Microscopy Sciences) and imaging was performed as previously described (Smith *et al.*, 2013), using a FEI Tecnai G^2 Spirit BioTWIN electron microscope with an AMT 2k CCD camera (XR60 model from Advanced Microscopy techniques).

Statistical analyses

Statistical analyses were performed with GraphPad Prism v6.05 (windows). All values are expressed as means +/− SEM. Two-tailed unpaired Student's T-test was used to compare a single measurement between two groups. one-way ANOVA followed by Dunnett's multiple comparisons post-hoc test was used for time course analysis of a single group. two-way ANOVA followed by Sidak's multiple comparisons post-hoc test were used for the analyses of time courses experiments comparing 2 groups. F-values, t-values and P-values are reported for each statistical test. In all tests $P \leq 0.05$ was considered significant.

Results

Functional sensory and motor recovery after sciatic nerve injury

First, we determined the sensory and motor functional recovery profiles of rats in two models of peripheral nerve injury one with rapid and the other with delayed regrowth (Fig. 1A). For rapid recovery we used the sciatic nerve crush model, in which the epineurium and perinurium remain intact (Figure 1A; Rich & Lichtman, 1989). In this model, we observed a full recovery of both sensory and motor function, as assessed by the pinprick test and SFI respectively (Fig. 1B, C). Recovery of the pinprick response started 10 days after the crush injury in the proximal hindpaw territory and was complete by postoperative day 27 (Fig. 1B). Motor recovery developed from postoperative day 20 and was complete by day 35 (Fig. 1C). The SFI index takes into account lateral and intermediate toe widths as well as foot print length and encompasses functional recovery of both the gastrocnemius and intraplantar muscles (Hare *et al.*, 1992). The return of all the rats to their pre-injury SFI values therefore indicates full recovery of motor coordination and function of the hindlimb, including the most distal paw muscles. This agrees with an extensive literature on this model.

For the delayed recovery model we performed a complete sciatic nerve transection followed by an immediate re-suture (Figure 1A; Ma *et al.*, 2011). After this injury where continuity of the nerve is disrupted, response to pinprick started to occur at postoperative day 20 and by postoperative day 55 every animal had fully recovered (Fig. 1D), suggesting that the resuture enabled injured axons to cross to the distal stump by putting the proximal and distal nerve in close proximity.

In marked contrast, however, the SFI remained at the lowest score at all time points tested (up to 90 days; Fig. 1E), indicating a failure of both gastrocnemius and intraplantar muscles to display signs of functional motor recovery. These results are comparable to the regeneration profile of mice in the same two injury models (Ma *et al.*, 2011) and in rats after traumatic nerve injuries (Terzis & Smith, 1987; Evans *et al.*, 1991). Somewhat surprisingly the onset of recovery for both sensory and motor responses occur at similar time points in both species, whereas the time required for full recovery is significantly longer in rats.

The lack of functional recovery after severe traumatic nerve injuries, such as a full nerve transection could be due to an insufficient numbers of motor fibers crossing the injury site. We therefore quantified the number of NF200-positive axons distal to the transection resuture injury (at the level of the ankle) and found no difference compared to the intact contralateral side (Fig. 1F). These results suggest that a large number of fibers can grow across a complete nerve section, which is compatible with the full sensory recovery observed in every animal.

We also compared the relative effects of a transection and resuture procedure performed in mice either distally (just below the sciatic notch) or proximally (just below the trifurcation) representing a ~1 cm difference (Fig. 2A). The degree of motor recovery of the gastrocnemius muscle was assessed using a grip strength test optimized for hindpaws. Mice with a more distal injury (closer to target tissue) displayed a partial return of grip strength while mice with the more proximal injury (further away to target tissue) failed to show this, indicating that a longer denervation time significantly attenuated the extent of functional recovery of the gastrocnemius muscle (Fig. 2B). We conclude that distance/time rather than the nature of the injury are the crucial factors for the success of motor recovery.

In our earlier mouse study we also concluded that denervation time was a critical factor in determining the ability to recover motor function, and estimated that this time window was approximately 35 days (Ma *et al.*, 2011). To further define the duration of the denervation period after which there is a failure of motor recovery, we designed a paradigm where mice were subjected to a sciatic nerve crush every week to produce different periods of denervation (Fig. 2C). Mice underwent a sciatic nerve crush every 7 days, a time too short for regenerating fibers to reach the gastrocnemius muscle (Fig. 2D). By performing 3, 4 or 5 crushes we were able therefore to denervate distal hindlimb muscles for approximately 24, 31 or 38 days (Fig. 2C). Sham controls received the same numbers of crushes but separated by a much shorter interval (2–3 days) and were capable of full sensory and motor recovery after the last crush (data not shown). After repeated crushes there was no obvious deficit in the numbers of regenerating fibers in the sciatic nerve compared to a single crush (Fig. 2E) and the extent of sensory recovery, assessed with pinprick, was similar in mice receiving 1

or 5 crushes (Fig. 2F). In contrast there was a gradual failure to recover motor function after multiple crushes, indicating a progressive defect of the gastrocnemius muscle to functionally recover with increasing denervation periods (Fig. 2G). This defect was even more pronounced for the distal intraplantar muscles, assessed by the toe spreading (TS) test (Fig. 2H). In mice that received 3 crushes, corresponding to a denervation period of approximately 24 days there was full recovery of the TS score within 2 weeks from the first onset of a positive response after the last crush, a profile superimposable with mice after a single crush. In mice that received 4 crushes, corresponding to an estimated denervation period of 31 days, the motor recovery was incomplete, as indicated by a maximum score only 50% of the pre-operative values, and this plateaued after 2–3 weeks from the first response. Finally in mice that received 5 crushes, which produced a denervation period estimated at 38 days there was virtually no recovery of the TS score. These results support the existence of a critical denervation period after which motor recovery is severely impaired. For intraplantar muscles in the mouse we estimate this period of denervation to be between 30 and 38 days. Interestingly, these experiments reveal an extremely sharp decrease in chances of motor recovery that occurs in the course of 2 weeks, from full recovery (24 days denervation) to no recovery (38 days denervation).

Anatomical Analyses

We next compared the anatomy of the NMJ of rats or mice that displayed full motor recovery after a single sciatic nerve crush with those with no recovery (transection and resuture or multiple crushes). The NMJ in intraplantar muscles were stained for NF200 (myelinated fibers) and α-bungarotoxin (that binds to the nicotinic AChR). Twelve weeks after transection and resuture injury in both species virtually all NMJ post-synaptic elements were contacted by NF200-positive fibers, indicating morphological full re-establishment of NMJ (Fig. 3A). Quantification of the number of re-innervated NMJ, assessed by colocalization of NF200 with α-bungarotoxin signals showed no difference between injured and non-injured muscles. In addition no major differences in the overall morphology of the NMJ or the arborization of the nerve fibers within the muscle were observed. Regenerating fibers displayed an increase in their volume-to-surface ratio, indicating an enlargement of the axon, as previously reported after prolonged denervation periods (Sulaiman & Gordon, 2000; Fig. 3B).

In the multiple crush model the vast majority of NMJs were re-innervated 12 weeks after the last crush, although some reduction was present in mice that received 5 crushes every 7 days (Fig. 3C, D). Because these animals were harvested 12 weeks after the last crush and never displayed any motor recovery, the post-synaptic element of NMJ likely remained non-functional for over 110 days (28 days after 5^{th} crush then 84 days of observation), allowing a partial declusterization of the AchR at the membrane (Frank *et al.*, 1975). This declusterization did not appear to be dependent on the number of crushes *per se*, as NMJ of mice that received 5 crushes every 2 or 3 days displayed full motor recovery and when harvested 12 weeks after the last crush did not show any defect in the morphology or intensity of α-bungarotoxin signal (Fig. 3C). We conclude that regenerating fibers reach and reform the NMJ and that the lack of functional recovery therefore is not caused by an inability of fibers to innervate the muscle.

Electron microscopy—To further analyze if the NMJ of animals with no motor recovery after prolonged denervation had any observable anatomical defect, we used electronic microscopy. Intraplantar muscles of rats were harvested 4 months after a transection and resuture injury. In NMJs examined from prolonged denervated muscle, the ultrastructural appearance of the NMJ was mostly normal, with the presence of axons in the correct location relative to the postsynaptic membrane, and containing many postsynaptic vesicles. The ultrastructure of the basal lamina and terminal Schwann cells resembled roughly that present in intact muscle, with no major morphological indication of axonal or Schwann cell retraction, or of failure to form a coincident presynaptic and postsynaptic junction. Myofibrils of denervated muscles had a weaker signal, as expected from a chronic lack of innervation. However, some NMJs in denervated muscles displayed a subsarcolemmal clustering of mitochondria at the postsynaptic site. In addition, there were increased number of large mitochondria with rarefied cristae in the axonal terminals. These characteristics are somewhat reminiscent of classic findings in myasthenia gravis (Woolf, 1966; Hong *et al.*, 2000), which might reflect or be a consequence of a possible defect in synaptic transmission (Fig. 4). We conclude that the lack of functional motor recovery in delayed reinnervated muscle models does not result from a lack of axon regeneration to the target or to a failure in the reestablishment by the regenerating axon to reform a structural synaptic apparatus at the correct site and with presence of presynaptic vesicles close to the normal release site and postsynaptic membrane.

Electrophysiological examination—To assess functional recovery of denervated muscles electrophysiologically, the compound muscle action potential (CMAP) evoked in response to sciatic nerve stimulation was recorded in both the gastrocnemius and intraplantar muscles 4 months postoperatively in rats. After a single crush, the delayed muscle latency and the amplitude of the CMAP in the gastrocnemius muscle recovered to levels equivalent to control intact muscles (Fig. 5A). In the intraplantar muscle, the latency showed a significant delay (5.0±0.23 ms compared to 3.5±0.13 ms in control; $t_{10}=5.56$, $P=0.000237$) indicating a likely delay in remyelination (Fig. 5A). After a transection and resuture sciatic nerve injury, the CMAP amplitude in the gastrocnemius muscle only reached 42% of that recorded from the intact contralateral side (11.7±2.3 mV compared to 26.0±4.1 mV in control muscle; $t_9=3.14$, $P=0.0118$) while for the ipsilateral intraplantar muscles the amplitude only reached 12% of that in the controls (0.7±0.2 mV vs 5.8±1.4mV; $t_9=3.89$, $P=0.0036$; Fig. 5B). Even though amplitude was very small, the latency was not that much greater than after a crush (gastrocnemius: 2.2±0.13 ms vs 1.6±0.18 ms; $t_9=2.75$, $P=0.02$; intraplantar 5.4±0.52 ms vs 3.04±0.43 ms; $t_9=3.37$, $P=0.0082$ when compared to contralateral muscle; $P=0.008$ when compared to crush condition; Fig. 5B). This suggests that in the transection and resuture model there is failure of restoration of functional NMJs that is distance and time dependent, but that remyelination does occur.

One reason for failure of motor function but not electrical activation could be severe muscle atrophy. H and E staining images from muscle contralateral and ipsilateral to the transection injury at 4 months, did not reveal obvious morphological features of atrophy, even though the muscles on the injured side were much smaller (Fig. 6A). Analysis of the distribution of type I (slow) fibers and type II (fast) fibers in gastrocnemius and intraplantar muscles

revealed changes consistent with the response of the muscle to prolonged denervation. Specifically type I (slow) fibers formed clusters in the gastrocnemius muscle in contrast to the evenly spread profile found in control muscles while the number of positive fibers was not changed (29.3 ± 5.83 % compared to 18.7 ± 1.70 % in control muscle; Fig.6B). In intraplantar muscles there was a significant increase in Type II (fast) fibers (94.3 ± 0.82 % compared with 85.5 ± 1.04 % in control muscle; $t_{17}=6.59$, $P=0.00004$) but no clusters (Fig. 6B).

In conclusion although motor axons are able to regenerate after many weeks into even distal muscles after a complete transection injury and re-establish NMJs with an apparent normal structure, there is a major failure of electrical activation of the muscle that correlates closely with the lack of functional motor recovery and we hypothesize that it is this synaptic failure that is a prime cause of the failure of motor recovery.

Discussion

In this study we sought to tease out the extent, timing and possible causes for poor motor recovery after peripheral nerve injury by comparing two models with high or low rates of functional recovery. Our results support the notion that in rodents, the absence of motor recovery after traumatic nerve injury is not necessarily due to a lack NMJ re-innervation or a retraction of motor axons after such regeneration, but rather to a defect in the ability to electrically activate the muscle.

Time as a critical factor for motor but not sensory functional recovery

Using a model of repeated nerve crushes to precisely modulate the denervation time, we estimate that in mice if return of motor function has not started by 30 days after injury, the chance of motor recovery drops severely, to become quasi null by postoperative day 38. We initially proposed a defect in terminal Schwann cells as a possible explanation for lack of motor recovery after transection and resuture injuries of the sciatic nerve in mice (Ma *et al.*, 2011). Surprisingly, we now find with better microscopy enabling a fine anatomical analysis of NMJs from intraplantar muscles of animals that failed to recover motor function, no apparent morphological defect compared to non-injured, functional NMJ. The results therefore do not support a failure to reach the NMJ, but rather suggest a defect in the transmission from motor axons to motor fibers. Indeed, CMAP recordings showed that these anatomically re-established NMJ are incapable of trigger normal muscle electrical activation, the key step in driving contraction, while the anatomy of the muscle itself does not show gross anatomical signs of atrophy. Previous studies have shown that muscles can still contract even after prolonged denervation periods (Ashley *et al.*, 2007; Carraro *et al.*, 2015). One limitation of CMAP recordings is that it represents the overall capacity of a muscle to respond to total nerve stimulation and does not allow for a precise analysis of neurotransmission. Electrophysiological studies of miniature and evoked endplate potentials are required to tease out the exact nature of the possible defect in NMJ activation and whether it reflects failure of transmitter content or release or the postsynaptic response to this.

In our repeated crush paradigm, where axons are prevented from reaching the muscle for defined times, we find that 38 days of denervation for intraplantar muscles results in failure of motor recovery. These results agree with our earlier finding, that if functional recovery has not started by day 35 after a transection and resuture injury in mice, motor recovery does not occur (Ma et al. 2011). These results imply a rapid change over time in the ability of axons and muscle to reform functional NMJs after peripheral nerve injury. Whereas peripheral nerve injury paradigms associated with disruption of the nerve integrity (section and resuture, grafts, silicon tubes) require regenerating fibers to cross a physical gap to reach their original target tissue, the multiple crush model does not disrupt the epineurium so that the main variable is the time of denervation. Using this paradigm we could switch a model considered 'favorable' for regeneration (crush injury) from full recovery to no recovery, despite no defect in neuronal growth, assessed by full sensory recovery and anatomical analyses of the NMJ. The critical period after multiple crushes and transection resuture injuries in mice is very similar, suggesting that in both models the lack of motor recovery is due to the duration of denervation, not the nature or severity of the injury. We now show that this is also true in rats where, although motor fibers also re-establish structural NMJs after a transection resuture injury, no functional motor recovery occurs.

Molecular factors involved in the establishment of functional NMJ

When an axon reaches the target muscle it needs to switch from an active growth state to one supporting synaptic maturation. Synaptic activity may be needed to consolidate a terminal differentiated state (Liu *et al.*, 2011). In the NMJ during development, target-derived factors such as FGFs, b2 laminin, and collagen a (IV) chains organize synaptogenesis by promoting differentiation of nerve terminals at synaptic sites (Fox *et al.*, 2007) and assembly of the motor endplate during early development depends on the interaction between agrin, which is synthetized by neurons and perisynaptic Schwann cells, and its receptor muscle-specific kinase (MuSK; Yang *et al.*, 2001; Wu *et al.*, 2010).

Whereas immediately after peripheral nerve injury terminal Schwann cells extend elaborate processes from the NMJ to guide the regenerating axons, they eventually begin to retract these processes and the degree of this retraction depends on the length of the period of denervation (Kang *et al.*, 2014). After prolonged denervation, muscle endplates also lose postsynaptic receptors, the size of muscle fibers decrease, and the ability of satellite cells to proliferate declines (Krasnova *et al.*, 1975; Anzil & Wernig, 1989; Kang *et al.*, 2014). It is possible therefore that a prolonged loss of NMJ function would cause both a contraction failure and a loss of the NMJ synaptic machinery. Matrix metalloproteinase 3 (MMP3), the major enzyme responsible for the degradation of agrin in denervated muscles is secreted by terminal Schwann cells and genetic deletion of MMP3 leads to sustained agrin levels in denervated muscle endplates (Chao et al., 2013). This promotes phosphorylation of MuSK which in turn preserves the integrity of motor endplates NMJ for at least 2 months following nerve degeneration, thereby allowing greater re-innervation (Chao *et al.*, 2013). It would be interesting to test if inhibiting MMP3 could extend the critical period in denervated animals and allow for more functional motor recovery after denervation periods longer than 38 days.

After peripheral nerve injury, the GTPase RhoA and the downstream Rho-kinase pathway is activated in motor neurons (but not Schwann cells) and inhibition of this pathway promotes motor fiber regeneration (Hiraga *et al.*, 2006), without affecting sensory fibers (Joshi *et al.*, 2015). *In vivo* pharmacological blockade of this pathway also improves myelination of motor fibers and increases the area of re-innervated NMJ (Joshi *et al.*, 2015). GTPase Rac1 and RhoA are also expressed by muscle cells where they are critical during development for the aggregation of AChR by agrin secreted by motor neurons (Reist *et al.*, 1992). Once activated Rac1 promotes the initial clustering of AChR and RhoA development of large clusters of AChR (Weston *et al.*, 2003). Interestingly RhoA levels increase in denervated muscles in the weeks following injury (Tsai *et al.*, 2011). This could lead to an imbalance in RhoA/Rac1, which would prevent optimal re-clustering of AchR upon re-innervation and activation by agrin, and therefore a failure of proper transmission.

Our observation of the presence of a normal ultrastructural appearance of the NMJ after prolonged denervation and reinnervation indicates that the lack of motor function is not due to the absence of either pre- or postsynaptic structural elements. Alteration in presynaptic vesicle content or release or an absence of postsynaptic responses to transmitter could account for the failure of functional NMJ reestablishment, and further study is required to reveal which mechanism is responsible and why.

Clinical implications of a critical period for re-establishing functional NMJ after nerve injury

In a clinical settings, motor functional recovery outcome from delayed (9–12 months) or late (>12 months) surgeries are extremely poor (Hoke, 2006). The current explanation for this is that the denervated muscle undergo irreversible changes in 12–18 months (Campbell, 2008) and in these cases, tendon transfers procedures or vascularized free muscle transfers are preferred over nerve repairs (Doi *et al.*, 2000; Giuffre *et al.*, 2010).

We show in this study in rodents that there is a critical period after which, even though regenerating fibers can still grow into the target muscle and reform NMJs, there is no functional motor outcome, and we hypothesize this is due to a synaptic defect, the nature of which now needs to be explored. The phenomenon of regrowth but not functional recovery precedes the well-described switch from a growth-permissive state to a non-growth-permissive one that occurs in muscles after long-term denervation, which prevents nerve regeneration and even promotes axon retraction (explaining why biopsies from extremely delayed repair surgeries are typically devoid of motor fibers).

Whether such a critical period after which where axons can recontact NMJs but fail to elicit contractions) exists in humans and how long it lasts before distal nerve become non-permissive, now needs to examined, since this could drive therapeutic interventions – especially once the molecular mechanisms responsible for motor synapse failure are identified.

Acknowledgments

Anthony Hill (IDDRC Cellular Imaging Core at Boston Children’s Hospital) for confocal microscope and axon analysis. Lai Ding (Enhanced Neuroimaging Core at Harvard Neuro Discovery Center) for analysis of NMJs

colocalized axons and the volume analysis soft with ImageJ. Matt Alexander at Boston Children's Hospital for suggestion of muscle fiber type staining protocol. The Harvard Medical School EM Facility. The Intellectual and Developmental Disabilities Research Center (IDDRC) of Children's Hospital (NIH P30 HD018655) for use of the Histology, Image Analysis and Animal Behavior Cores. **CJW:** Dr. Miriam and Sheldon G. Adelson Medical Research Foundation, NIH 2 R01 NS038153-15 and the Bertarelli Foundation. **MS:** funded by Yonemitsu foundation at Kumamoto Kino Hospital. **AL** was partially supported by RO1DE022912 grant. **SH** was funded by BCH Pathology T32 training grant (5T32HL110852-03).

References

Anzil AP, Wernig A. Muscle fibre loss and reinnervation after long-term denervation. Journal of neurocytology. 1989; 18:833–845. [PubMed: 2621479]

Ashley Z, Sutherland H, Lanmuller H, Russold MF, Unger E, Bijak M, Mayr W, Boncompagni S, Protasi F, Salmons S, Jarvis JC. Atrophy, but not necrosis, in rabbit skeletal muscle denervated for periods up to one year. Am J Physiol Cell Physiol. 2007; 292:C440–451. [PubMed: 17218372]

Asplund M, Nilsson M, Jacobsson A, von Holst H. Incidence of traumatic peripheral nerve injuries and amputations in Sweden between 1998 and 2006. Neuroepidemiology. 2009; 32:217–228. [PubMed: 19174611]

Buchthal F, Kuhl V. Nerve conduction, tactile sensibility, and the electromyogram after suture or compression of peripheral nerve: a longitudinal study in man. Journal of neurology, neurosurgery, and psychiatry. 1979; 42:436–451.

Campbell WW. Evaluation and management of peripheral nerve injury. Clin Neurophysiol. 2008; 119:1951–1965. [PubMed: 18482862]

Carlstedt T, Grane P, Hallin RG, Noren G. Return of function after spinal cord implantation of avulsed spinal nerve roots. Lancet. 1995; 346:1323–1325. [PubMed: 7475770]

Carraro U, Boncompagni S, Gobbo V, Rossini K, Zampieri S, Mosole S, Ravara B, Nori A, Stramare R, Ambrosio F, Piccione F, Masiero S, Vindigni V, Gargiulo P, Protasi F, Kern H, Pond A, Marcante A. Persistent muscle fiber regeneration in long term denervation. Past, present, future. European journal of translational myology. 2015; 25:77–92. [PubMed: 25844146]

Chao T, Frump D, Lin M, Caiozzo VJ, Mozaffar T, Steward O, Gupta R. Matrix metalloproteinase 3 deletion preserves denervated motor endplates after traumatic nerve injury. Annals of neurology. 2013; 73:210–223. [PubMed: 23281061]

Doi K, Muramatsu K, Hattori Y, Otsuka K, Tan SH, Nanda V, Watanabe M. Restoration of prehension with the double free muscle technique following complete avulsion of the brachial plexus. Indications and long-term results. J Bone Joint Surg Am. 2000; 82:652–666. [PubMed: 10819276]

Evans PJ, Bain JR, Mackinnon SE, Makino AP, Hunter DA. Selective reinnervation: a comparison of recovery following microsuture and conduit nerve repair. Brain Res. 1991; 559:315–321. [PubMed: 1794104]

Fox MA, Sanes JR, Borza DB, Eswarakumar VP, Fassler R, Hudson BG, John SW, Ninomiya Y, Pedchenko V, Pfaff SL, Rheault MN, Sado Y, Segal Y, Werle MJ, Umemori H. Distinct target-derived signals organize formation, maturation, and maintenance of motor nerve terminals. Cell. 2007; 129:179–193. [PubMed: 17418794]

Frank E, Gautvik K, Sommerschild H. Cholinergic receptors at denervated mammalian motor end-plates. Acta physiologica Scandinavica. 1975; 95:66–76. [PubMed: 1180105]

Fu SY, Gordon T. Contributing factors to poor functional recovery after delayed nerve repair: prolonged axotomy. The Journal of neuroscience : the official journal of the Society for Neuroscience. 1995; 15:3876–3885. [PubMed: 7751952]

Fu SY, Gordon T. The cellular and molecular basis of peripheral nerve regeneration. Molecular neurobiology. 1997; 14:67–116. [PubMed: 9170101]

Gallo G. RhoA-kinase coordinates F-actin organization and myosin II activity during semaphorin-3A-induced axon retraction. Journal of cell science. 2006; 119:3413–3423. [PubMed: 16899819]

Giuffre JL, Kakar S, Bishop AT, Spinner RJ, Shin AY. Current concepts of the treatment of adult brachial plexus injuries. The Journal of hand surgery. 2010; 35:678–688. quiz 688. [PubMed: 20353866]

Griffin JW, Pan B, Polley MA, Hoffman PN, Farah MH. Measuring nerve regeneration in the mouse. Experimental neurology. 2010; 223:60–71. [PubMed: 20080088]

Hare GM, Evans PJ, Mackinnon SE, Best TJ, Bain JR, Szalai JP, Hunter DA. Walking track analysis: a long-term assessment of peripheral nerve recovery. Plastic and reconstructive surgery. 1992; 89:251–258. [PubMed: 1732892]

Hiraga A, Kuwabara S, Doya H, Kanai K, Fujitani M, Taniguchi J, Arai K, Mori M, Hattori T, Yamashita T. Rho-kinase inhibition enhances axonal regeneration after peripheral nerve injury. J Peripher Nerv Syst. 2006; 11:217–224. [PubMed: 16930283]

Hoke A. Mechanisms of Disease: what factors limit the success of peripheral nerve regeneration in humans? Nature clinical practice Neurology. 2006; 2:448–454.

Hoke A, Gordon T, Zochodne DW, Sulaiman OA. A decline in glial cell-line-derived neurotrophic factor expression is associated with impaired regeneration after long-term Schwann cell denervation. Experimental neurology. 2002; 173:77–85. [PubMed: 11771940]

Hong SM, Khang SK, Kim KK, Bae Y, Park SH. A case of myasthenia gravis proven by ultrastructural study. J Korean Med Sci. 2000; 15:251–254. [PubMed: 10803708]

Jessen KR, Mirsky R. Signals that determine Schwann cell identity. Journal of anatomy. 2002; 200:367–376. [PubMed: 12090403]

Joshi AR, Bobylev I, Zhang G, Sheikh KA, Lehmann HC. Inhibition of Rho-kinase differentially affects axon regeneration of peripheral motor and sensory nerves. Experimental neurology. 2015; 263:28–38. [PubMed: 25261755]

Kang H, Tian L, Mikesh M, Lichtman JW, Thompson WJ. Terminal Schwann cells participate in neuromuscular synapse remodeling during reinnervation following nerve injury. The Journal of neuroscience : the official journal of the Society for Neuroscience. 2014; 34:6323–6333. [PubMed: 24790203]

Kawamura DH, Johnson PJ, Moore AM, Magill CK, Hunter DA, Ray WZ, Tung TH, Mackinnon SE. Matching of motor-sensory modality in the rodent femoral nerve model shows no enhanced effect on peripheral nerve regeneration. Experimental neurology. 2010; 223:496–504. [PubMed: 20122927]

Krasnova IN, Trager R, Ved'mina EA, Ogneva NS, Ibragimov F. Typing of vibrions by specific O-sera. Zhurnal mikrobiologii, epidemiologii, i immunobiologii. 1975:37–41.

Liu K, Tedeschi A, Park KK, He Z. Neuronal intrinsic mechanisms of axon regeneration. Annual review of neuroscience. 2011; 34:131–152.

Luo L, O'Leary DD. Axon retraction and degeneration in development and disease. Annual review of neuroscience. 2005; 28:127–156.

Ma CH, Omura T, Cobos EJ, Latremoliere A, Ghasemlou N, Brenner GJ, van Veen E, Barrett L, Sawada T, Gao F, Coppola G, Gertler F, Costigan M, Geschwind D, Woolf CJ. Accelerating axonal growth promotes motor recovery after peripheral nerve injury in mice. J Clin Invest. 2011; 121:4332–4347. [PubMed: 21965333]

Millesi H, Meissl G, Berger A. The interfascicular nerve-grafting of the median and ulnar nerves. J Bone Joint Surg Am. 1972; 54:727–750. [PubMed: 4560075]

Oberlin C, Beal D, Leechavengvongs S, Salon A, Dauge MC, Sarcy JJ. Nerve transfer to biceps muscle using a part of ulnar nerve for C5-C6 avulsion of the brachial plexus: anatomical study and report of four cases. The Journal of hand surgery. 1994; 19:232–237. [PubMed: 8201186]

Reist NE, Werle MJ, McMahan UJ. Agrin released by motor neurons induces the aggregation of acetylcholine receptors at neuromuscular junctions. Neuron. 1992; 8:865–868. [PubMed: 1316763]

Reynolds ML, Woolf CJ. Terminal Schwann cells elaborate extensive processes following denervation of the motor endplate. Journal of neurocytology. 1992; 21:50–66. [PubMed: 1346630]

Rich MM, Lichtman JW. In vivo visualization of pre- and postsynaptic changes during synapse elimination in reinnervated mouse muscle. The Journal of neuroscience : the official journal of the Society for Neuroscience. 1989; 9:1781–1805. [PubMed: 2542480]

Ruijs AC, Jaquet JB, Kalmijn S, Giele H, Hovius SE. Median and ulnar nerve injuries: a meta-analysis of predictors of motor and sensory recovery after modern microsurgical nerve repair. Plastic and reconstructive surgery. 2005; 116:484–494. discussion 495–486. [PubMed: 16079678]

Saito H, Dahlin LB. Expression of ATF3 and axonal outgrowth are impaired after delayed nerve repair. BMC neuroscience. 2008; 9:88. [PubMed: 18801180]

Smith IW, Mikesh M, Lee Y, Thompson WJ. Terminal Schwann cells participate in the competition underlying neuromuscular synapse elimination. The Journal of neuroscience : the official journal of the Society for Neuroscience. 2013; 33:17724–17736. [PubMed: 24198364]

Son YJ, Thompson WJ. Schwann cell processes guide regeneration of peripheral axons. Neuron. 1995; 14:125–132. [PubMed: 7826630]

Sulaiman OA, Gordon T. Effects of short- and long-term Schwann cell denervation on peripheral nerve regeneration, myelination, and size. Glia. 2000; 32:234–246. [PubMed: 11102965]

Terenghi G. Peripheral nerve regeneration and neurotrophic factors. Journal of anatomy. 1999; 194(Pt 1):1–14. [PubMed: 10227662]

Terzis JK, Smith KJ. Repair of severed peripheral nerves: comparison of the “de Medinaceli” and standard microsuture methods. Experimental neurology. 1987; 96:672–680. [PubMed: 3556204]

Tsai FC, Pai MH, Chiu CC, Chou CM, Hsieh MS. Denervation dynamically regulates integrin alpha7 signaling pathways and microscopic structures in rats. J Trauma. 2011; 70:220–227. [PubMed: 21268308]

Tsuyama N, Hara T, Maehiro S, Imoto T. Intercostal nerve transfer for traumatic brachial nerve palsy. Seikei Geka. 1969; 20:1527–1529. [PubMed: 5393194]

Vuorinen V, Siironen J, Roytta M. Axonal regeneration into chronically denervated distal stump. 1. Electron microscope studies. Acta neuropathologica. 1995; 89:209–218. [PubMed: 7754742]

Weston C, Gordon C, Teressa G, Hod E, Ren XD, Prives J. Cooperative regulation by Rac and Rho of agrin-induced acetylcholine receptor clustering in muscle cells. J Biol Chem. 2003; 278:6450–6455. [PubMed: 12473646]

Woolf AL. Morphology of the myasthenic neuromuscular junction. Ann N Y Acad Sci. 1966; 135:35–59. [PubMed: 5221350]

Wu H, Xiong WC, Mei L. To build a synapse: signaling pathways in neuromuscular junction assembly. Development. 2010; 137:1017–1033. [PubMed: 20215342]

Yang JF, Cao G, Koirala S, Reddy LV, Ko CP. Schwann cells express active agrin and enhance aggregation of acetylcholine receptors on muscle fibers. The Journal of neuroscience : the official journal of the Society for Neuroscience. 2001; 21:9572–9584. [PubMed: 11739568]

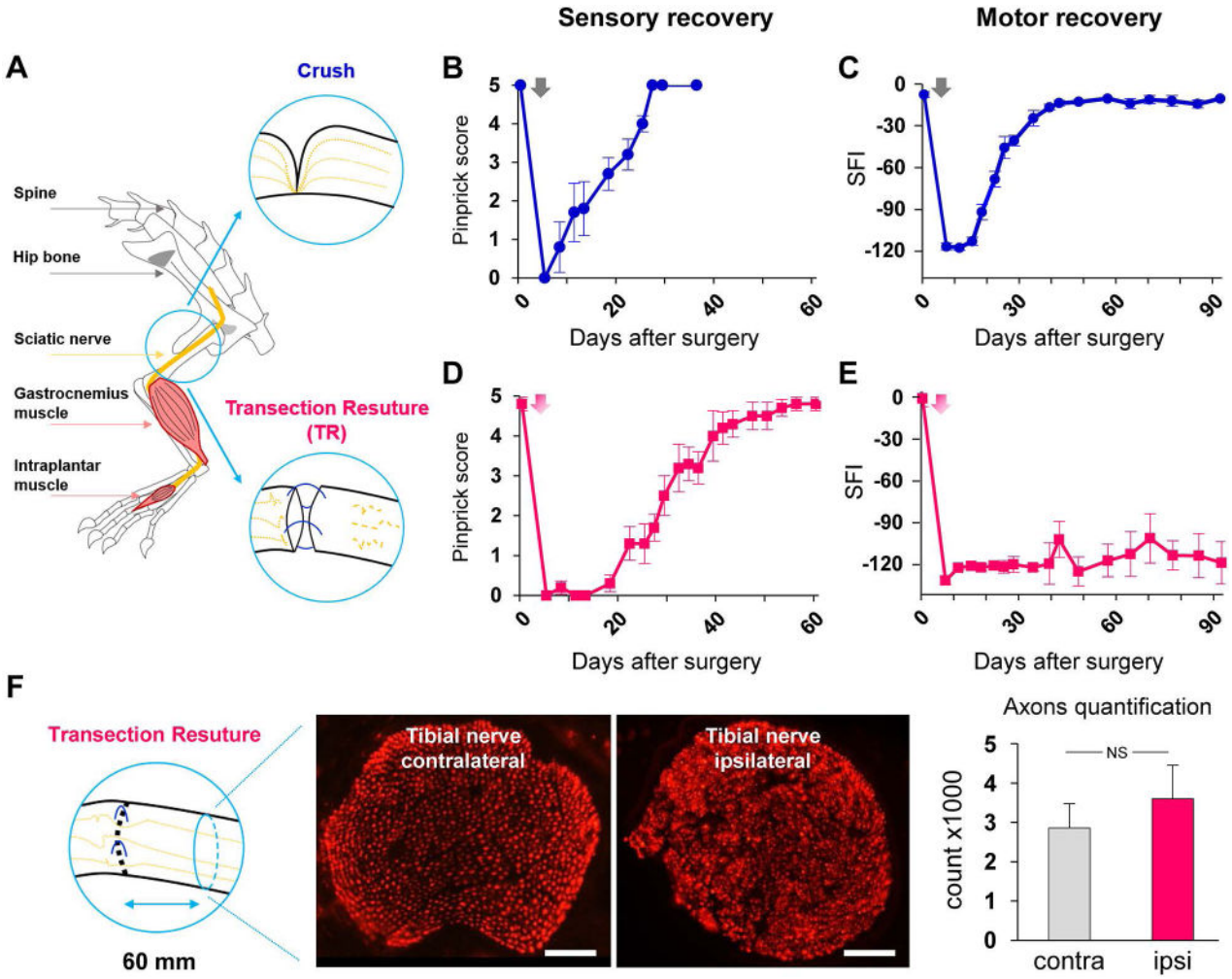

Figure 1. Sensory and motor functional recovery in two models of peripheral nerve injuries in rats

A) Rats underwent either sciatic nerve crush (top, blue) which leaves epineurium and perinurium intact to support nerve growth, or sciatic nerve transection and resuture (bottom, pink) after which regenerating fibers need to cross the injury site and re-contact target tissues. The main muscles innervated by the sciatic nerve involved in hindpaw movement are the gastrocnemius and the intranplantar muscles. B, C) **Sciatic nerve crush:** B) Pinprick response score (0 = no response and 5 = response in every region of the plantar skin) and C) SFI (assessed by DigiGait; a score of −100 and below corresponds to total paralysis whereas uninjured animals typically have a score of −8.8 or above) tested at various times after injury. Every animal recovered both sensory and motor functions. D, E) **Sciatic nerve transection and resuture**: D) Pinprick response score and E) SFI tested at various times after injury. Whereas there is a return of sensory function in every animal, there was no motor recovery. The arrow indicates the time of injury (N=6 per group). F) Representative immunostaining and quantification of the total number of axons in transverse tibial nerve sections (60 mm distal from crush site) immunostained for NF200 in naïve condition and after transection and resuture. There are no significant statistic difference between the axons number of the both sides. Scale bar represents 100μm.

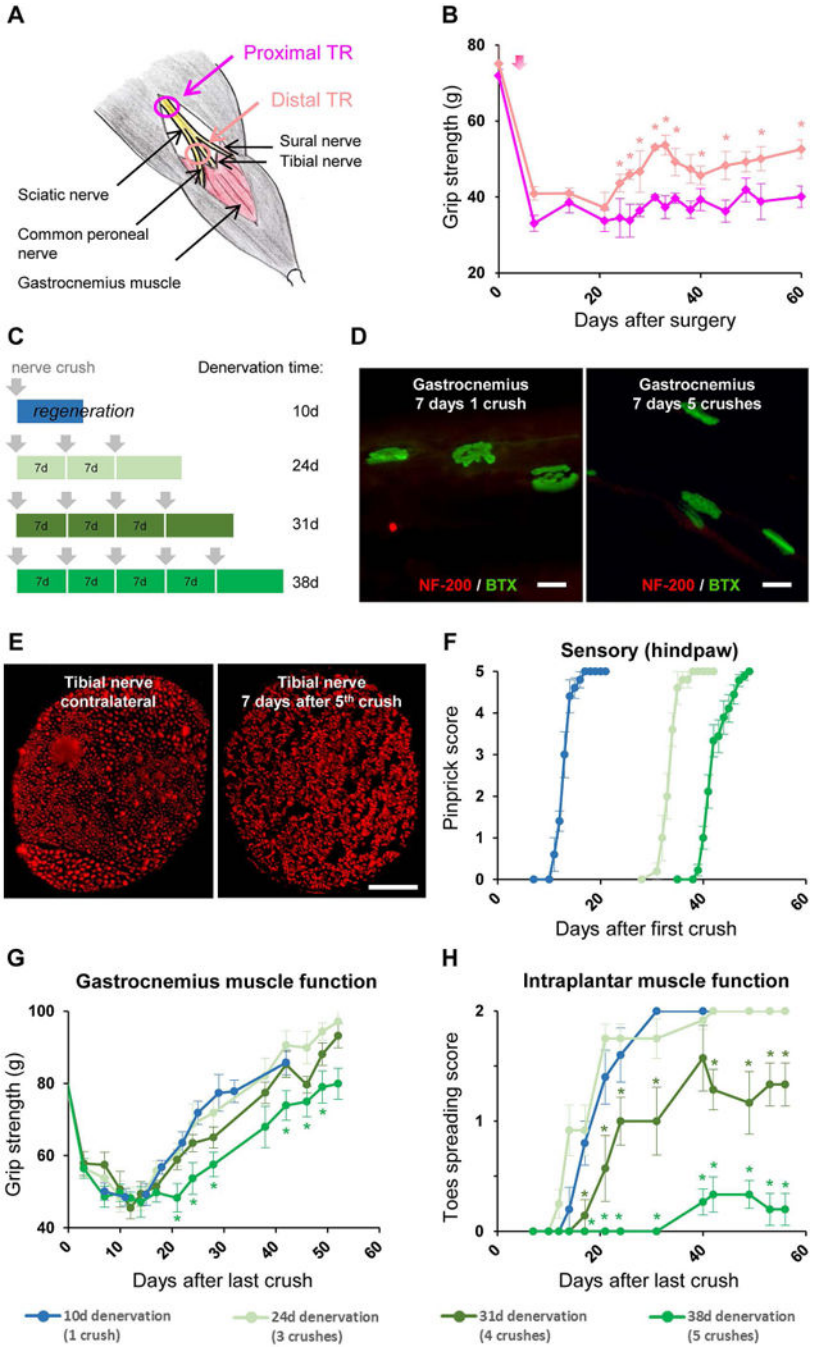

Figure 2. Prolonged muscle denervation time severely reduces the chances of motor recovery

A) Schematic representation of the proximal versus distal transection and resuture paradigm. Proximal injury of the sciatic nerve was performed just below the sciatic notch (pink) and distal injury just below the trifurcation (salmon). B) Motor recovery of the hindpaw was assessed by grip strength at various times after injury in mice. Animals with a distal injury displayed partial motor recovery, in contrast to the more proximal injury. C) Schematic representation of the multiple crushes paradigm. A sciatic nerve crush was performed every seven days 3, 4 or 5 times. The estimated time to reach the distal target tissues is 10 days

('regeneration'). Accordingly the denervation time is dependent on the number of crushes: 24d, 31d or 38d. D) Gastrocnemius sections stained for NF200 (red) and FITC-conjugated α-bungarotoxin (green) 7 days after a single crush or 5 crushes. No fibers were detected in the muscles. Scale bar represents 50 μm. E) Representative pictures of transverse tibial nerve sections immunostained for NF200 (red) from an uninjured nerve or 7 days after 5 crushes. Scale bar represents 50 μm. F) Pinprick response score in mice after various denervation periods (i.e. number of crushes). In all conditions every mouse fully recovered. G) Assessment of gastrocnemius muscles function using grip strength (in g) of the hindpaws after various denervation periods (i.e. number of crushes) in mice. After 3 crushes mice fully return to pre-injury grip strength values within 35–40 days, whereas 4 and 5 crushes cause a progressive deficit in recovery. H) Assessment of intraplantar muscles function using toes spreading score (0 no spreading, 1 transient spreading and 2 full and sustained spreading of the toes) after various denervation periods (i.e. number of crushes) in mice. After 3 crushes (24 days denervation period) mice fully recover the toes spreading reflex with a time course similar to after a single crush. When mice are denervated for 31 days the recovery is partial and after 38 days no toes spreading responses were observed. (N=3–8 per group). *$p<0.05$ two-way ANOVA followed by Sidak's multiple comparisons post-hoc compared with proximal (B) ($F(1,5)=16.92$, $P=0092$) or 1x crush (G: 5 crushes: $F(1,13)=6.535$, $P=0.02$ and H: 4 crushes: $F(1,17)=16.96$, $P=0.0007$; 5 crushes: $F(1,25)= 220.4$, $P<0.0001$).

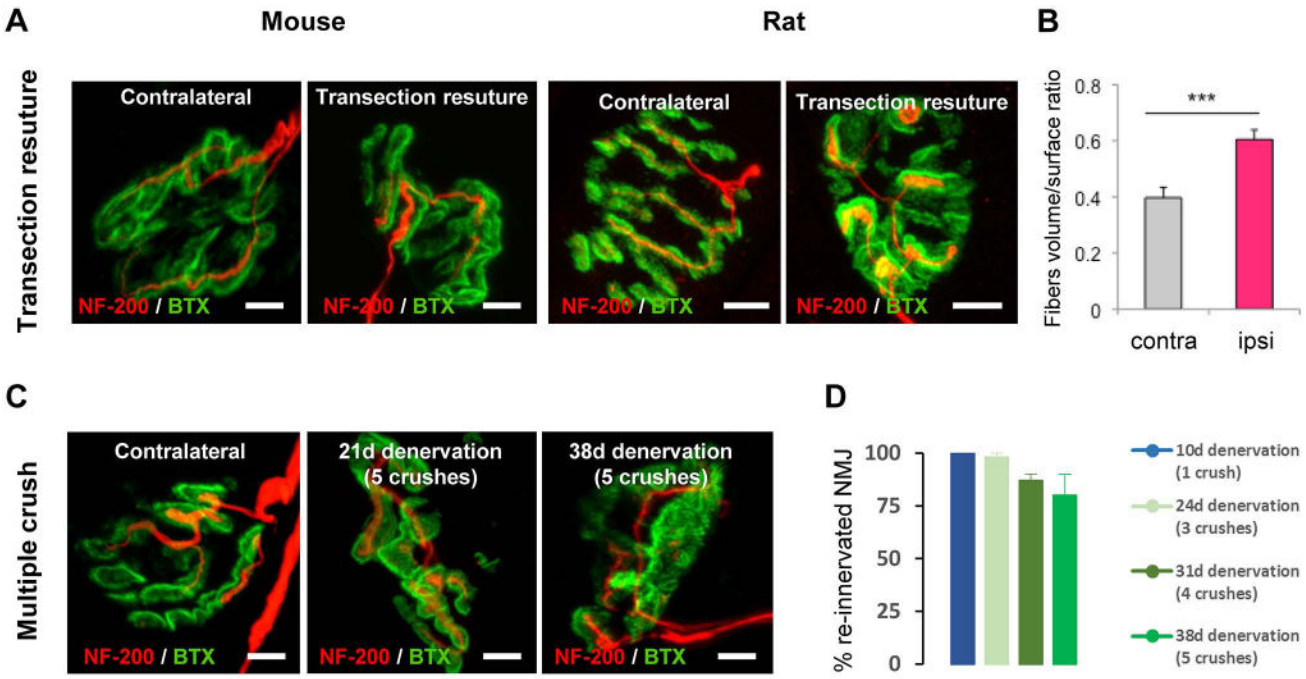

Figure 3. Confocal imaging of NMJ after sciatic nerve injuries

A) Representative sections of intraplantar muscles sections (20 μm) stained for NF200 (red) and FITC-conjugated α-bungarotoxin (green) after transection and resuture injury in mice (3 months after surgery) and rats (4 months after surgery). Every NMJ sampled co-localized with NF200-positive fibers. B) Analysis of the ratio volume / surface of the red signal (NF200) overlapped with green signal (α-bungarotoxin) analyzed by 3D images on ImageJ. There is an increase in axonal volume compared to control muscles in rats. *$P<0.0001$ Two-tailed unpaired Student's T-test. C) Representative sections of intraplantar muscles sections (20 μm) stained for NF200 (red) and FITC-conjugated α-bungarotoxin (green) 8 weeks after multiple crushes injury in mice. D) Quantification of the percentage of NMJ re-innervated in mice after multiple crushes. Scale bar represents 50 μm. (N=6 each group and 10 sections per animal).

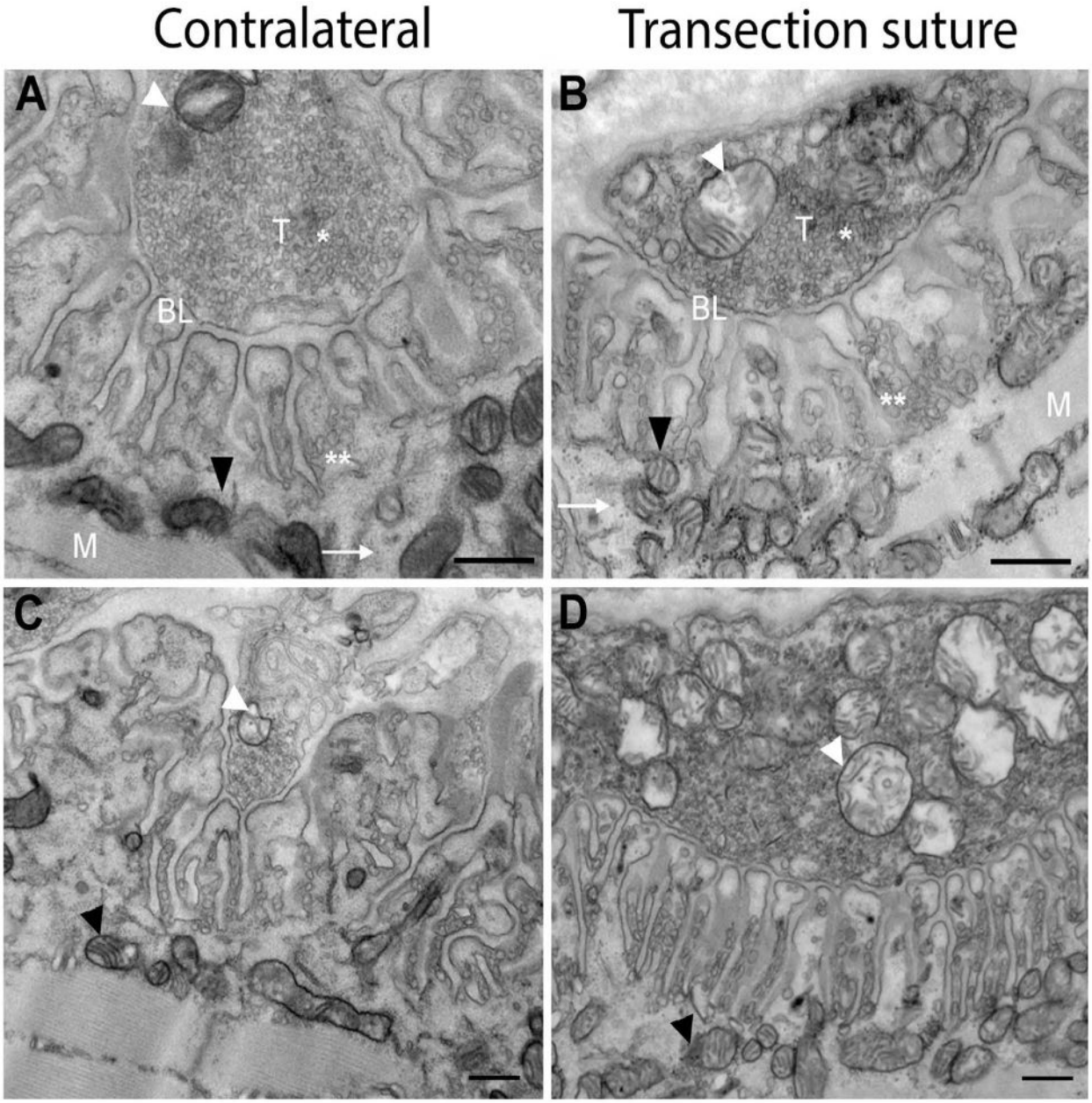

Figure 4. Ultrastructure of NMJ after injury

Representative EM image of intraplantar muscle in control condition (left, A and C) or 4 months after transection and resuture (right, B and D). Note the difference in mitochondria. **Key:** T: axon terminal; BL: basal lamina; M, muscle fibers; *, presynaptic vescle; **, postsynaptic vesicle; black arrow head: postsynaptic/subsarcolemmal mitochondria; white arrow head: axonal terminal mitochondria; white arrow: acetylcholine. Scale bars: 500 nm.

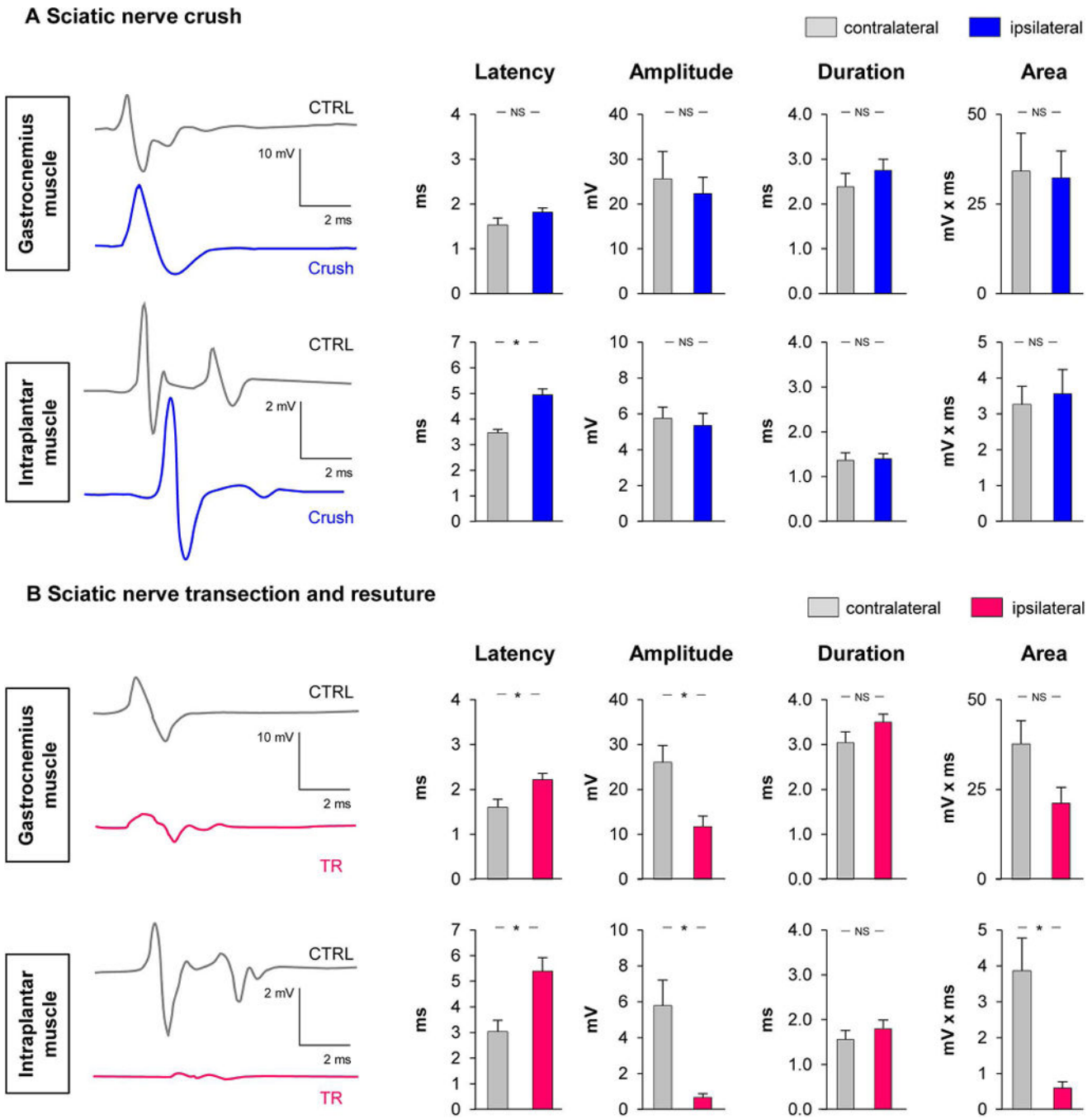

Figure 5. Electrophysiological properties of gastrocnemius and intraplantar muscles 4 months after sciatic nerve crush (A) or transection and resuture (B) injury

Representative CMAP recordings from gastrocnemius and intraplantar muscles evoked by sciatic nerve stimulation below trifurcation in control (gray) and 4 months after nerve injury (blue: crush, pink: transection and resuture). A) After sciatic nerve crush, there is a full recovery of CMAP parameters in the gastrocnemius muscle. In the intraplantar muscle amplitude and duration are restored, and there is an increased latency. B) After transection and resuture there is a significant drop in amplitude for the gastrocnemius muscle. In the intraplantar muscle, there is an increased latency but also a significant reduction in

amplitude and area of CMAP. N=6 per group. *$P<0.05$ Two-tailed unpaired Student's T-test (values displayed in text).

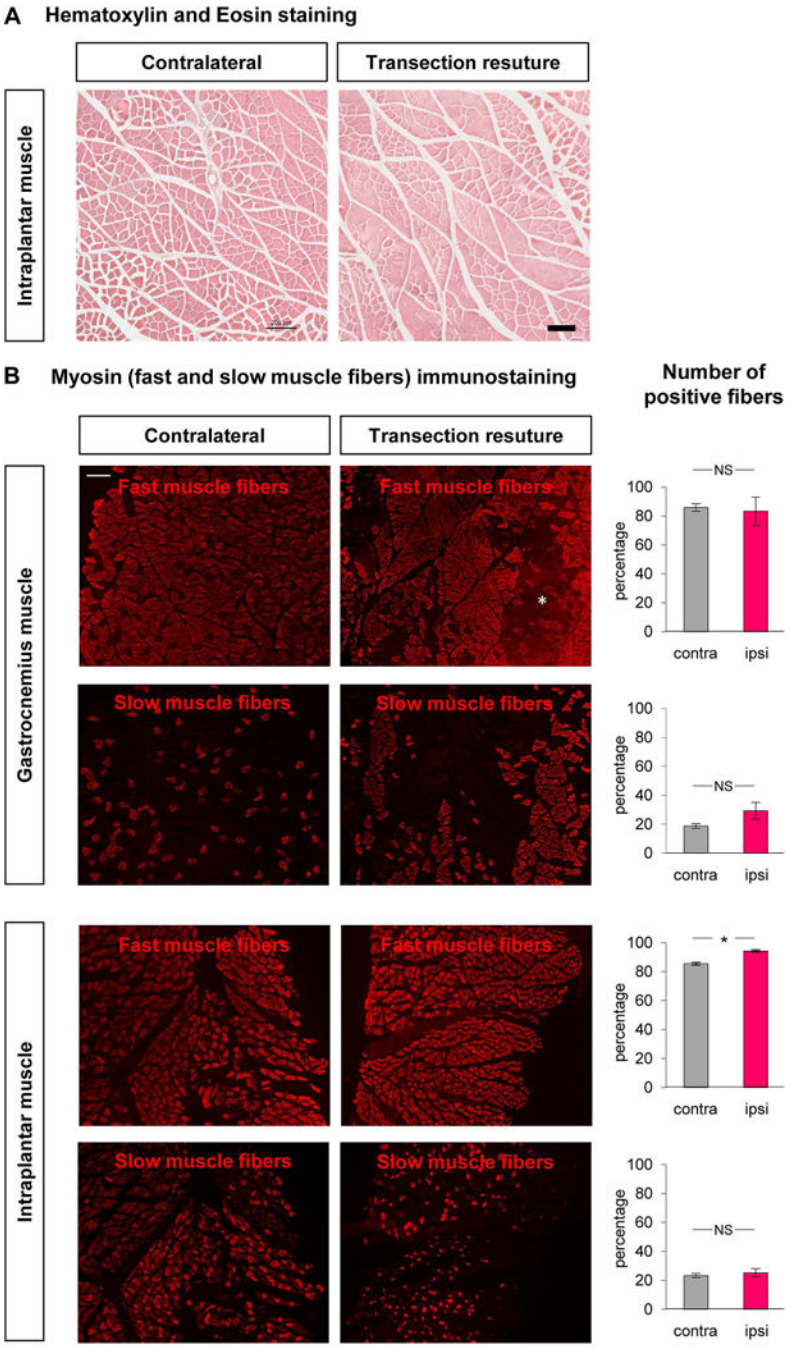

Figure 6. Muscle fiber immunohistochemistry

A) Hematoxylin and eosin staining of intraplantar muscle in control condition and 4 months after transection and resuture injury. B) Gastrocnemius and intraplantar muscles immunostained against fast- and slow-myosin in control condition and 4 months after transection and resuture injury and quantification of the proportion of slow- and fast-myosin-positive fibers. * in gastrocnemius muscle image indicates an area of clustered myosin fibers in the muscle 4 months after transection and resuture injury, something not observed in control muscles. In intraplantar muscles there is a significant increase in Type II

(fast) fibers after injury ($p<0.00005$). N= 4–6 animals per group; 500–2000 fibers counted. *$p<0.05$* Two-tailed unpaired Student's T-test (values displayed in text).